

SYNTHESIS AND CHARACTERIZATION OF SILVER NANOPARTICLES BY EXTRACTED EUGENOL (AgNPE) FROM *Ocimum sanctum* L. LEAF (KALAR-PIN-SEIN)

Su Thiri Kyaw¹, Myo Maung Maung², Mya Kay Thi Aung³

Abstract

Ocimum sanctum L. (holy basil) leaves were collected from Hpa-an Township, Kayin State and verified its botanical name at Department of Botany, Hpa-an University. The isolation of eugenol from holy basil (Kalar-pin-sein) leaves was carried out by distillation method, followed by adding NaCl (to separate aqueous layer and organic layer), NaOH (to form sodium ion in place of H⁺ of its hydroxyl group), acidified by HCl (protonating eugenolate moiety that gives eugenol), adding Na₂SO₄ (to dehydrate at all) and separated by adding hexane to give mostly pure eugenol. The characterization of extracted eugenol was studied by TLC, UV, FT IR and GC-MS methods. The R_f value was found at 0.56 (hexane : acetone, 9:1 v/v) and it was UV active. The wavelength of maximum absorption was found to be 285 nm. It was soluble in petroleum ether, ethyl acetate, chloroform, methanol and ethanol but insoluble in water. This was also confirmed by the broad O-H stretching band at 3520 cm⁻¹ and aromatic C-O stretching bands between 1200-1270 cm⁻¹ in FT IR spectrum. GC-MS identified the prepared sample as eugenol definitely with strong molecular ion peak at m/z 164 accompanied by diagnostic fragment peaks which are identical with the reported spectrum. Synthesis of silver nanoparticles by extracted eugenol (AgNPE) and characterization in association of average and single crystallite sizes calculation by X-ray diffraction were also studied. A cost effective and environmental friendly method has been carried out for green synthesis of silver nanoparticles (AgNPE) from different volumes (8 and 10 mL) of silver nitrate solution (1.0 mM) as metal precursor. From indexing XRD patterns, it could be confirmed that the optimal synthesized AgNPE-8 and AgNPE-10 had face-centered cubic (FCC) crystal system because of the indices with all odd or all even numbers. It was observed that the average crystallite sizes of AgNPE-8 and AgNPE-10 were respectively by found to be 42.03 nm and 34.93 nm according to Scherrer formula. From the results, it could be deduced that the prepared AgNPE had the properties of nanoparticles.

Keywords : *Ocimum sanctum* L., holy basil leaves, distillation, eugenol, silver nanoparticles, Scherrer equation, face-centered cubic

¹ 3PhD, Candidate, Assistant Lecturer, Department of Chemistry, Hpa-an University

² Lecturer, Department of Chemistry, Dagon University

³ Lecturer, Department of Chemistry, University of Yangon

Introduction

Nanotechnology is concerned with the synthesis of nanoparticles of variable sizes, shapes and chemical composition and their use for human benefits (Kaur *et al.*, 2013). Silver nanoparticles (AgNPs) have emerged as an outstanding product from the field of nanotechnology because of their unique properties such as good conductivity, chemical stability, catalytic properties, electrical and magnetic properties, which can be incorporated into antimicrobial applications, biosensor materials, composite fibres, cosmetic products and electronic components (Mukherjee *et al.*, 2001; Sondi and Salopek-Sondi, 2004). Plant and plant extracts have shown a great potential for the synthesis of AgNPs because they possess a broad variety of metabolites like flavones, ketones, terpenoids, aldehydes, amides and carboxylic acids responsible for the bioreduction process involved in the synthesis (Kaur *et al.*, 2013).

Nowadays, the use of different types of medicinal plants has been increased by traditional medical practitioners for the treatments of various types of diseases. The most common and important medicinal plant i.e., *Ocimum sanctum* L. which has different medicinal properties such as anticancer, antimicrobial, cardio-protective, antidiabetic, analgesic, antispasmodic, antiemetic, hepatoprotective, antifertility, adaptogenic and diaphoretic actions.

The active constituent of leaves of the *O.sanctum* is eugenol (1-hydroxy-2-methoxy-4-allylbenzene) which is mainly responsible for the therapeutic potentials of cardiovascular system, urinary system, reproductive system, immune system, gastric system, blood biochemistry, central nervous system and also significance in various ailments in modern medicine (Mondal *et al.*, 2009; Hemaiswarya *et al.*, 2008; Raseetha *et al.*, 2009). The essential oil of any herb can be extracted by using a variety of methods including distillation, solvent extraction, cold pressing, maceration or supercritical carbon dioxide extraction.

Nanoparticles are generally characterized by their size, shape, surface area and dispersity (Jiang *et al.*, 2009). The common techniques of characterizing nanoparticles are UV-visible spectrophotometry, Fourier

transform infrared spectroscopy (FT IR) and powder X-ray diffraction (XRD) (Shahverdi *et al.*, 2011).

The UV-visible spectroscopy is a commonly used technique (Pal *et al.*, 2007). Light wavelengths in the 300-800 nm are generally used for characterizing various metal nanoparticles in size range of 2 to 100 nm. FT IR spectroscopy is useful for characterizing the surface chemistry (Chithrani *et al.*, 2006). XRD is used for the phase identification of the crystal structure of the nanoparticles (Sun *et al.*, 2000).

AgNPs have strong antimicrobial activities and can attack at the same time a broad range of targets in microorganisms, such as proteins with thiol groups, cell walls and cell membranes. AgNPs show antimicrobial activities against various infectious organisms, e.g., *Escherichia coli*, *Bacillus subtilis*, *Staphylococcus aureus*, *Pseudomonas aeruginosa* and *Vibrio cholerae* (Kim *et al.*, 2009; Narasimha *et al.*, 2011).

Due to their antimicrobial activity, AgNPs can play a promising role in food packaging system to prevent the growth of fouling contaminants and to improve the shelf life of food. In therapeutic treatment AgNPs display cytoprotective activity against HIV-1 infected cells. In water and air filters they can be incorporated into apparels, foot wears, paints, wound dressings, appliances, cosmetics and plastics (Sun *et al.*, 2005; Sharma *et al.*, 2009; Kannan and Subbalaxmi, 2011).

Materials and Methods

Collection of *Ocimum sanctum* Leaves

Freshly green leaves of *O.sanctum* (Kalar-pin-sein) were collected from Hpa-an in Kayin State and identified by authorized botanists at Botany Department, Hpa-an University.

Preparation of Dry Powder of *Ocimum sanctum* Leaves

O.sanctum (Kalar-pin-sein) leaves were thoroughly washed with double distilled water. After washing with water, the collected samples were dried at room temperature. The dried samples were cut into small pieces and ground into powder by grinding machine. These powder samples were stored

in the air-tight container to prevent moisture changes and contamination before analysis.

Extraction of Eugenol

Dry powder (10 g) and distilled water (100 mL) were mixed and distilled until approximately 50 mL of oily distillate was collected. NaCl (3 g) was added to the distillate and let to cool down. The organic compound drives into organic layer and transferred to separatory funnel where 25 mL of hexane was added and shaken to extract the organic oils from the aqueous layer and shaken and vent to release pressure. After 5 min of shaking, there were two layers formed, the bottom aqueous layer was drained and discarded. Then, 25 mL of 10 % NaOH solution was added followed by shaking, venting and discarding the upper organic layer. The aqueous layer was acidified using 6 M HCl. The acidified aqueous layer was placed back in the separatory funnel. 25 mL of hexane was added, repeating the same shaking and venting process for 5 min. The bottom aqueous layer was discarded and the upper organic layer was transferred to a conical flask. Then a small amount of anhydrous Na₂SO₄ was added and swirled. The extract (eugenol) were obtained.

Characterization of some Physical Properties of the Extracted Compound

The extracted compound was characterized by determination of physical properties: R_f value and solubilities in various solvents as shown in Table 1.

Determination of R_f values of the Extracted Compound

The extracted compound was subjected to TLC analysis and the R_f value of the spot was determined. GF₂₅₄ silica gel precoated aluminium plate (Merck) was employed. After the plate was dried, the R_f value of extracted compound was measured. Localization of spot was made by viewing directly under UV lamp (254 and 365 nm). The R_f value observed for extracted compound was then recorded. The chromatogram of extracted compound is shown in figure 2.

Determination of Solubilities of the Extracted Compound

The extracted compound was taken to determine its solubilities in some organic solvents such as pet-ether, chloroform, ethyl acetate, ethanol and methanol.

Identification of the Extracted Compound

The extracted compound was structurally identified by modern spectroscopic techniques such as UV-visible, FT IR and Mass spectroscopy.

Study on UV-visible Spectrum of the Extracted Compound

The UV-visible absorption spectrum of the extracted compound was recorded on a UV-visible Spectrophotometer (Shimadzu) at the West Yangon University.

Study on FT IR Spectrum of the Extracted Compound

The infrared spectrum of extracted compound was recorded and examined by using FT IR spectrophotometer (Perkin Elmer Spectrum GX Fourier Transform Infrared Spectrophotometer) at Universities' Research Centre, YU. The extracted compound was sampled with KBr pellet.

Study on Mass Spectrum of the Extracted Compound

For the identification of extracted compound, the mass spectrum was recorded and examined the molecular weight and the structural features of the compound. The mass spectrum of extracted compound was recorded by GC-MS mass spectrometer at the West Yangon University.

Preparation of 1 mM AgNO₃ Solution

Silver nitrate solution (1 mM solution) was prepared by adding 0.0169 g of AgNO₃ in deionized water in the 100 mL conical flask and the volume was made up to the mark.

Synthesis of Colloidal Solution of Silver Nanoparticles

Colloidal solutions of silver nanoparticles were synthesized in accordance with the following procedure.

Different volumes (5, 10, 15, 20 and 25 μ L) of the extracted compound was typically added to 2, 4, 6, 8 and 10 mL of silver nitrate solution (1 mM)

respectively to reduce Ag^+ ion to Ag^0 (nanoparticles). The colloidal solution of silver nanoparticles colouring colloidal brown was obtained within an hour (for about 50 min). The solution was allowed to at room temperature overnight. The colloidal solutions obtained were stored in refrigerator until further use to analyse.

Confirmation for the Existence of Silver Nanoparticles in Solution by Tyndall Effect

A laser pointer was taken and wrapped a rubber band around the on-switch so it was on continuously. The laser pointer was placed to the edge of the bottles containing AgNP colloidal solution and the light was passed through the solution. The observation was recorded. The laser pointer was then rotated at 90° intervals and recorded any new observations. The photograph of observation about the existence of silver nanoparticles in solution are represented in Figure 1.

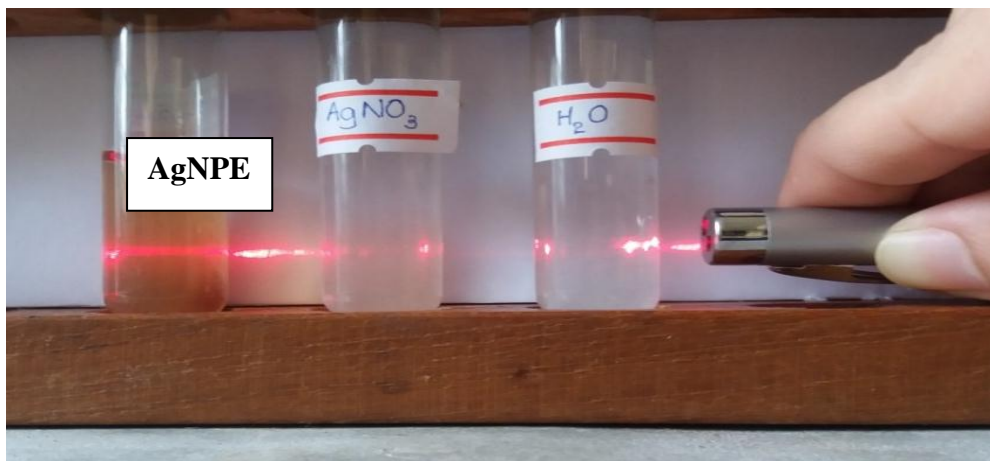


Figure 1: Dispersion of light (by laser beam) through AgNPs in aqueous medium

Confirmation of the Formation and the Presence of Silver Nanoparticles (a Colloidal Solution) by the Spectra of the UV-Visible Spectrophotometry

The sample solutions were first diluted with distilled water. The UV-visible spectroscopic measurements of the silver nanoparticles were carried

out by a computer controlled on a UV-visible Spectrophotometer (Shimadzu) at the West Yangon University.

Confirmation of the Functional Groups of Silver Nanoparticles by FT IR Spectroscopy

The characterization of functional groups of silver nanoparticles was investigated by FT IR analysis (Shimadzu) and the spectrum was scanned in the range of 4000-400 cm^{-1} . The samples were prepared by dispersing the silver nanoparticles uniformly in a matrix of dry KBr, compressed to form an almost transparent disc. KBr was used as a standard analyse the samples. The recorded spectrum is shown in Figure 8 and the band assignments of silver nanoparticles are presented in Table 3.

Determination of Crystallite Size by Using Scheerer's Formula and Identification of Structure of Prepared Silver Nanoparticles by using XRD Diffractograms

The synthesized colloidal AgNPE solution was incubated at room temperature for about 2 days. After 2 days, the solution was observed to have distinctly deposited precipitate at the bottom of flask, leaving the colloidal supernatant at the top. The upper aliquot (colloidal AgNPE) was decanted and stored in refrigerator for further use. The precipitated silver nanoparticle powder was obtained and it was designated as AgNPE-8 and AgNPE-10 respectively according to their concentrations.

The samples of silver nanoparticle powder (AgNPE-8 and AgNP-10) were analysed by X-ray diffraction technique to identify the crystallite size and structure. The recommended procedure used was in accordance with the catalogue.

The XRD spectra of the AgNPE-8 and AgNPE-10 are presented in Figures 9 and 10. The average crystallite size of AgNPE samples was calculated by using Scherrer's formula.

$$L = \frac{K \lambda}{\beta \cos \theta}$$

where, L = average crystallite size
K = constant related to crystallite shape

λ	=	wavelength of X-ray radiation $\text{CuK}\alpha_1$
β	=	Full width at half maximum of 2θ
θ	=	diffraction Bragg angle

Tables 4 and 5 show the average cryatsllite size of prepared silver nanoparticles.

Results and Discussion

R_f values of the Extracted Compound

The extracted compound was subjected by TLC. After the plate was dried, the R_f value of extracted compound was measured. Localization of spot was made by viewing directly under UV lamp. The R_f value of extracted compound in respective solvent system is reported in Table 1.



Figure 2: TLC chromatogram of extracted compound

Solubilities of the Extracted Compound

The extracted compound was taken to determine their solubilities in some organic solvents such as pet-ether, chloroform, ethyl acetate, ethanol and methanol. This result is recorded in Table 1.

Table 1: Characterization of some Physical Properties of Extracted Compound

Test		Extracted Compound
	R _f value	0.56
	Solvent system	Hexane : acetone (9:1 v/v)
	Yield %	0.159
Solubility	PE	+
	CHCl ₃	+
	EtOAc	+
	EtOH	+
	MeOH	+

(+) = soluble

Identification of the Extracted Compound by Modern Spectroscopic Techniques

After characterization, the extracted compound was generally classified and then were identified by modern spectroscopic techniques such as UV-visible, FT IR and GC-MS spectroscopy.

The UV-visible spectrum (Figure 3) of the extracted compound in methanol showed the maximum absorption wavelength at 285 nm with high intensity indicating the presence of conjugated double bonds.

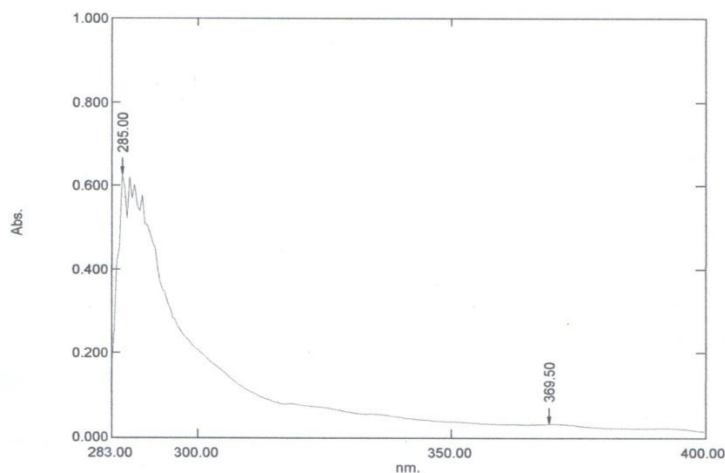


Figure 3: UV spectrum of the extracted compound (in methanol)

The functional groups in the extracted compound was studied by FT IR spectroscopy. The observed FT IR spectrum and spectral data assignment are presented in Figure 4 and Table 2, respectively. The broad band at 3520 cm^{-1} indicated the presence of O-H group and it appeared due to O-H stretching vibration. The presence of aromatic ring could be confirmed by the band at 3066 cm^{-1} appeared due to aromatic = C – H stretching. The bands observed at 1606 , 1512 and 1446 cm^{-1} was assigned to aromatic C = C stretching, the peaks at 1271 and 1226 cm^{-1} were assigned due to C-O-C stretching of aromatic C-O stretching of phenol. All of these observations indicated the presence of phenolic group in extracted compound.

In addition, the bands at 2968 , 2897 and 2835 cm^{-1} appeared due to asymmetric and symmetric stretching of O-CH₃ group, respectively. The absorption bands at 912 , 808 and 748 cm^{-1} were attributed to C-H out of plane bending of 1, 2, 4 trisubstituted aromatic ring.

Consequently, from the FT IR spectrum data, the extracted compound could be assumed to possess phenolic group and O-CH₃ group.

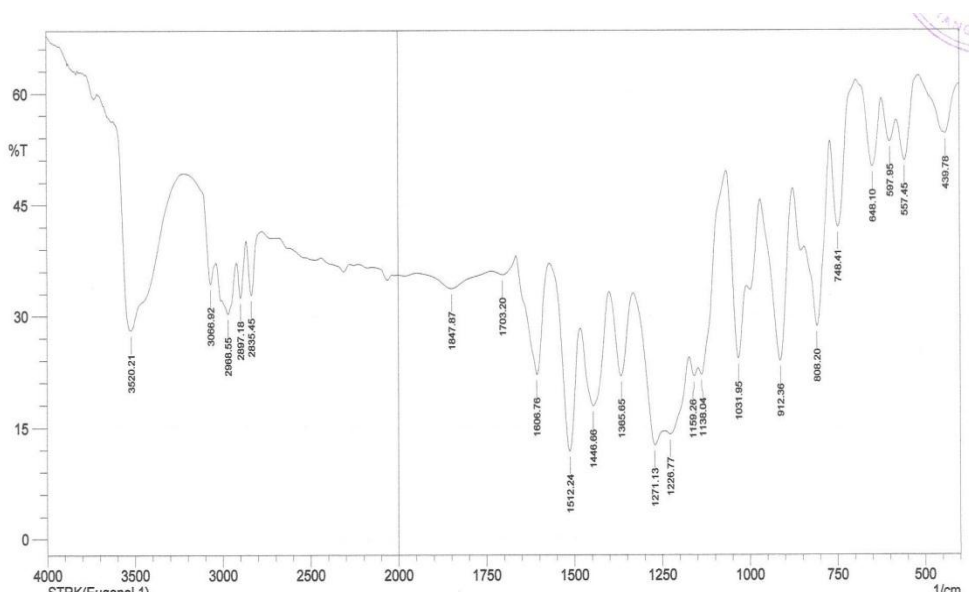
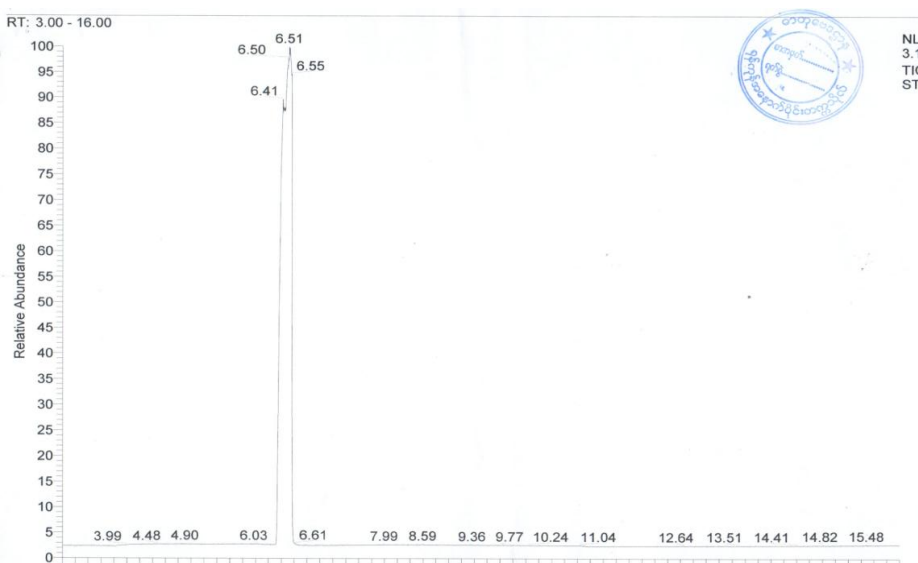


Figure 4: FT IR spectrum of the extracted compound

Table 2: FT IR Spectral Data of Extracted Compound

Wavenumber (cm ⁻¹)	vibrational mode	Assignment
3520	$\nu_{\text{O-H}}$	-OH stretching
3066	$\nu_{\text{=C-H}}$	= C - H stretching
2968, 2897, 2835	$\nu_{\text{C-H}}$ (asy, sym)	- CH ₃ and CH ₂
1606	$\nu_{\text{C=C}}$	C = C stretching
1512, 1446	$\nu_{\text{C=C}}$	C = C of aromatic ring
1365	δ_{CH_3} (sym)	-CH ₃ symmetric bending
1271, 1226	$\nu_{\text{C-O-C}}$ (asy)	C-O-C stretching of alkoxy aromatic ether and aromatic C-O stretching of phenol
1031, 912	$\delta_{\text{oop=C-H(vinyl)}}$	=C-H oop. bending of vinyl group
912, 808, 748	$\delta_{\text{oop ar C-H}}$	C-H out of plane bending of 1, 2, 4 trisubstituted aromatic ring

**Figure 5: GC chromatogram of the extracted eugenol**

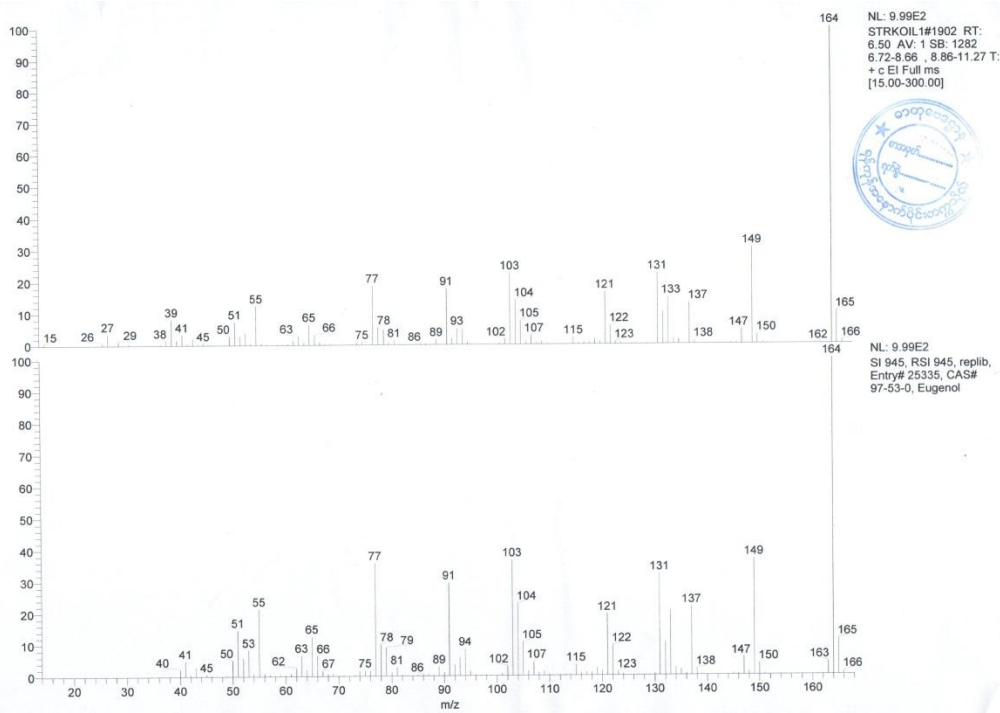
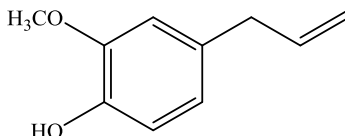


Figure 6: GC-MS spectrum of the extracted eugenol at retention time 6.50 min

The structure of the extracted compound was studied by GC-MS spectroscopy. Figure 5 illustrates the GC chromatogram and the MS spectrum at retention time 6.50 min is presented in Figure 6. In MS spectrum, the molecular ion peak was observed at $m/z = 164$ and the fragmentation pattern is the same as that of eugenol, indicating that the extracted compound has the molecular mass of 164. Therefore, the extracted compound was molecular mass 164 and molecular formula $C_{10}H_{12}O_2$.

From the about overall observation, the extracted compound could be identified as eugenol.



Eugenol (extracted compound)

Existence of Silver Nanoparticles in Solution Studied by Tyndall Effect

The Tyndall effect is the scattering of light as a light beam passes through the colloid. Figure 1 shows the existence of silver nanoparticles in aqueous solution (as colloids). This Tyndall effect could be evident that the colloids have dispersed particles, making them nanoparticles. Hence, the particles will not settle out of the mixture.

According to this evidence, it was found that laser beam does not pass through water and silver nitrate solution. The dispersion of light passes through AgNPE in aqueous medium.

Confirmation of Colloidal AgNPE in Aqueous Solution by UV-Visible Spectrophotometry

UV-visible spectroscopy is a valuable tool for structural characterization of silver nanoparticles.

Figure 7 shows the UV absorption spectrum of colloidal AgNPE. It indicated that the silver nanoparticles were formed in aqueous phase, being stable with no precipitation. The maximum UV-visible absorption peak of colloidal AgNPE was appeared at 279 nm.

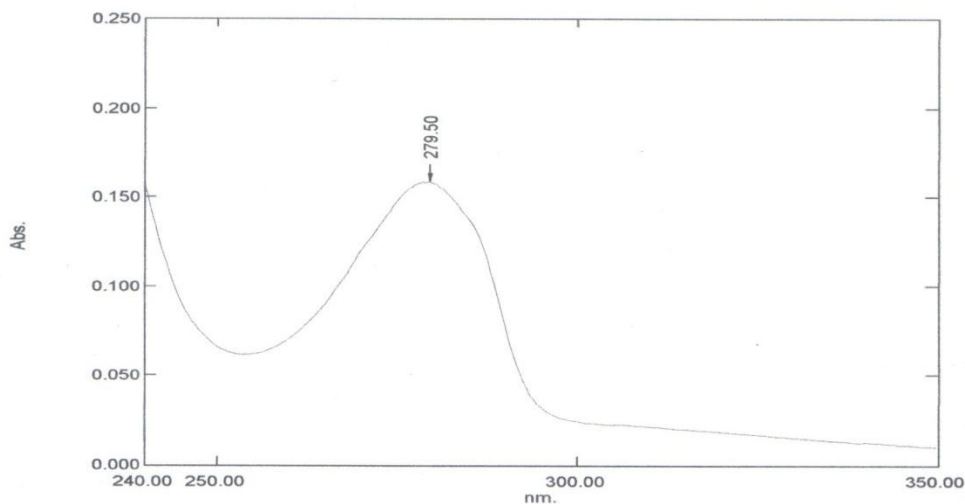


Figure 7: UV spectrum of colloidal silver nanoparticles (in methanol)

Confirmation of the Functional Groups of Silver Nanoparticles by FT IR Spectrophotometry

FT IR measurements were carried out to identify the biomolecules for capping and efficient stabilization of the metal nanoparticles synthesized. The observed FT IR spectrum and spectral data assignment of silver nanoparticles are presented in Figure 8 and Table 3, respectively.

The bands at 3348 cm^{-1} and 3361 cm^{-1} corresponds to O-H stretching of alcohols and phenols. The peak found that 1636 cm^{-1} and 1647 cm^{-1} showed C=O stretching of conjugated system.

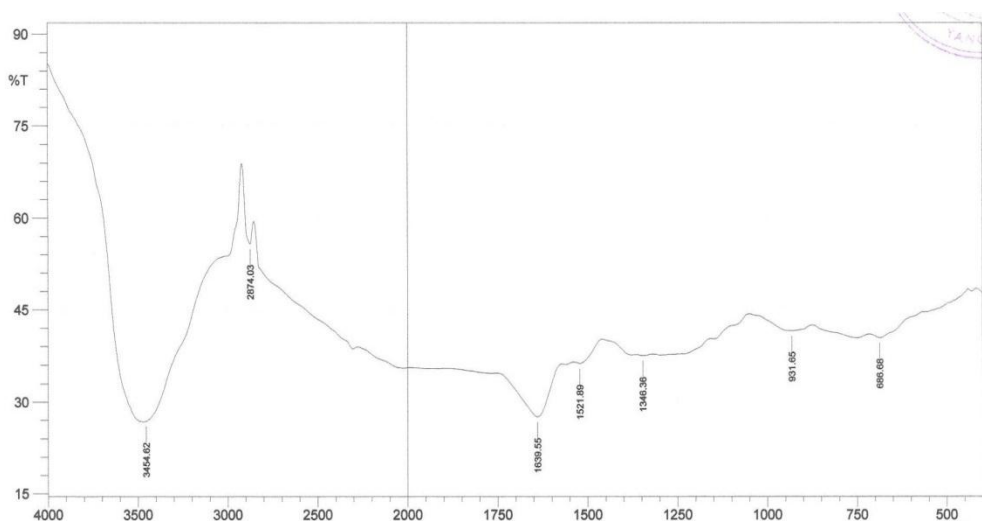


Figure 8: FT IR spectrum of colloidal silver nanoparticles

Table 3. FT IR Spectral Data of Silver Nanoparticles

Wavenumber (cm^{-1})	vibrational mode	Assignment
3455	$\nu_{\text{O-H}}$	-OH stretching of H-bonded alcohols and phenols
2874	$\nu_{\text{C-H}}$ (asy, sym)	- CH_3 and CH_2
1640	$\nu_{\text{C=C}}$	C = C stretching
1522	$\nu_{\text{C=C}}$	C = C of aromatic ring
1346	δ_{CH_3} (sym)	- CH_3 symmetric bending

Structure of the Prepared Silver Nanoparticles and the Crystallite Size by Using Debye-Scheerer's Formula from X-Ray Diffractograms

Figures 9 and 10 represent the X-ray diffractograms of the AgNPE-8 and AgNPE-10 and Tables 4 and 5 describe the average crystallite size with respect to their relating parameters of 2θ , d and FWHM (the full-width at half maximum). The Bragg reflections corresponding to the (1 1 1), (2 0 0) and (2 2 0) sets of lattice planes were observed from the patterns.

These Miller indices corresponding to the (1 1 1), (2 0 0) and (2 2 0) showed all-odd or all-even sets of lattice planes which could be designated as the face-centred cubic (FCC) structure of silver nanoparticle.

The average crystallite sizes of silver nanoparticles were calculated using Debye-Scheerer's formula. The average crystallite sizes of AgNPE-8 and AgNPE-10 were respectively found to be 42.03 nm and 34.93 nm from the measurements of X-ray diffraction (XRD) respectively. From the results, it could be deduced that the prepared silver nanoparticles had the properties of nanoparticles confirmed by the characterization.

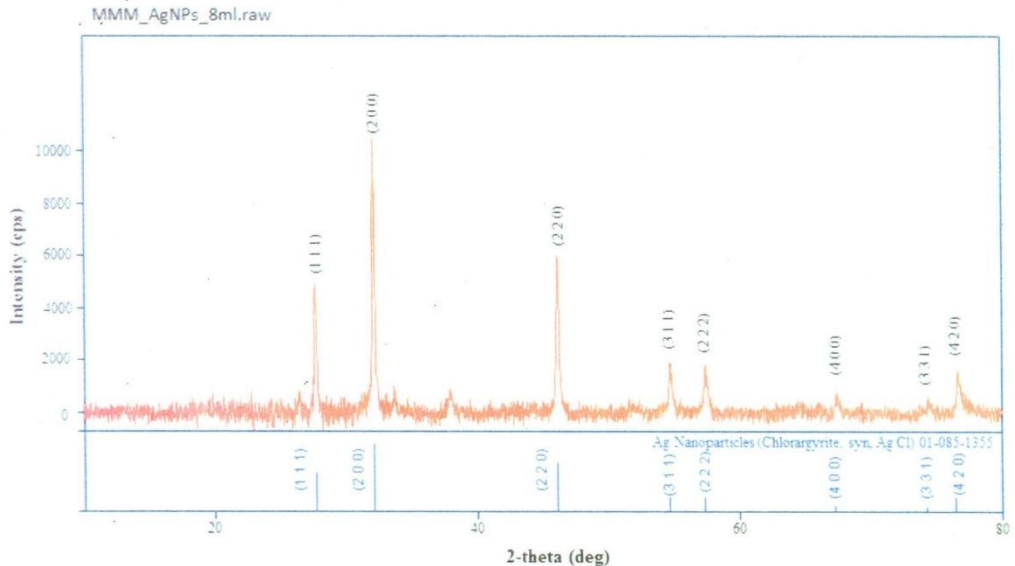


Figure 9: X-ray diffractogram of AgNPE-8

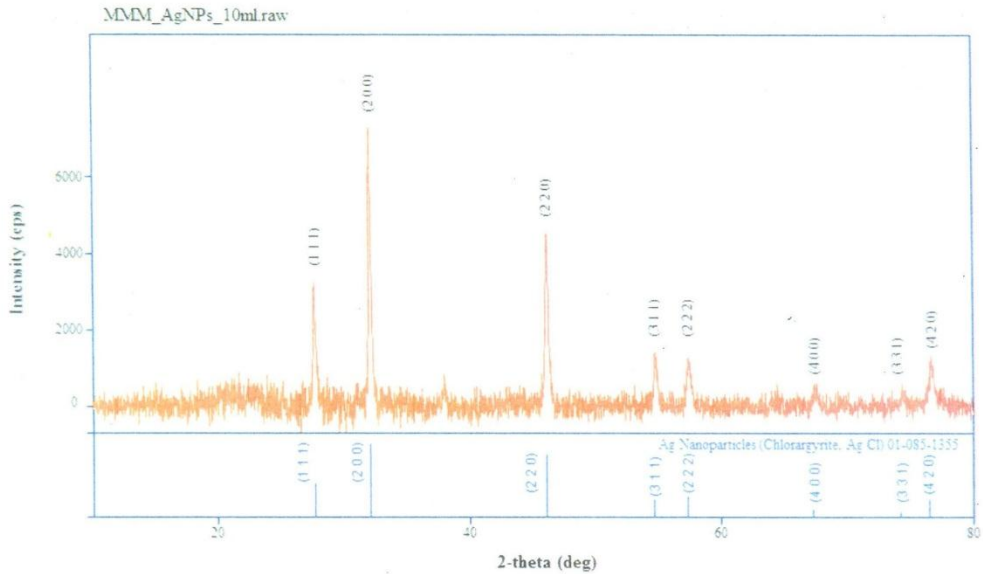


Figure 10: X-ray diffractogram of AgNPE-10

Table 4: Data for Calculation of Average Crystallite Size of AgNPE-8

Peak	2 θ (deg)	θ (deg)	cos θ	β of FWHM (deg)	β (rad)	L (nm)
1	27.7297	13.8649	0.9764	0.1512	0.002631	53.99
2	32.1272	16.0636	0.9683	0.1632	0.002840	50.44
3	46.0732	23.0366	0.9352	0.1982	0.003449	43.00
4	54.6274	27.3137	0.9094	0.2184	0.003800	40.14
5	57.2749	28.6375	0.9005	0.2246	0.003901	39.48
6	67.2023	33.6012	0.8639	0.2477	0.004310	37.25
7	74.1791	37.0896	0.8350	0.2642	0.004597	36.13
8	76.4468	38.2234	0.8251	0.2696	0.004691	35.83
Average crystallite size, L =						42.03

Table 5: Data for Calculation of Average Crystallite Size of AgNPE-10

Peak	2 θ (deg)	θ (deg)	cos θ	β of FWHM (deg)	β (rad)	L (nm)
1	27.7375	13.8688	0.9764	0.2195	0.003819	37.20
2	32.1363	16.0682	0.9683	0.2176	0.003786	37.83
3	46.0866	23.0433	0.9352	0.2246	0.003908	37.95
4	54.6437	27.3219	0.9093	0.2400	0.004176	36.53
5	57.2921	28.6461	0.9005	0.2466	0.004291	35.50
6	67.2233	33.6117	0.8638	0.2791	0.004856	33.07
7	74.2030	37.1015	0.8349	0.3096	0.005387	30.84
8	76.4717	38.2359	0.8250	0.3209	0.005584	30.11
Average crystallite size, L =						34.93

Conclusion

Ocimum sanctum L. (holy basil) leaves having positive and sound benefits have to be used in synthesis of silver nanoparticles. The isolation of eugenol from *O. sanctum* leaves were carried out by distillation method. The characterization of extracted eugenol was studied by TLC, UV, FT IR and GC-MS methods. The R_f value was found at 0.56 (hexane : acetone, 9:1v/v) and it was UV active. The wavelength of maximum absorption was found to be 285 nm. It was soluble in petroleum ether, ethyl acetate, chloroform, methanol and ethanol but insoluble in water. This was also confirmed by the broad O-H stretching band at 3520 cm^{-1} and aromatic C-O stretching bands between $1200\text{-}1270\text{ cm}^{-1}$ in FT IR spectrum. GC-MS identified the prepared sample as eugenol definitely with strong molecular ion peak at m/z 164 accompanied by diagnostic fragment peaks which are identical with the reported spectrum. From indexing XRD patterns, it could be confirmed that the optimal synthesized AgNPE-8 and AgNPE-10 had face-centered cubic (FCC) crystal system because of the indices with all odd or all even numbers. It was observed that the average crystallite sizes of AgNPE-8 and AgNPE-10 were respectively found to be 42.03 nm and 34.93 nm according to Scherrer formula. From the results, it could be deduced that the prepared AgNPE had the properties of nanoparticles.

Acknowledgements

The authors would like to express their profound gratitude to the Department of Higher Education (Yangon Office), Ministry of Education, Myanmar for provision of opportunity to do this research.

References

- Chithrani, B.D., Ghazani, A.A. and Chan, W.C.W. (2006). "Determining the Size and Shape Dependence of Gold Nanoparticle Uptake into Mammalian Cells". *Nano Lett*, vol 6(4), pp 662-668
- Hemaiswarya, S., Kruthiventi, A.K. and Doble, M. (2008). "Synergism between Natural Products and Antibiotics against Infectious Diseases". *Phytomedicine*, vol 15, pp 639-652
- Jiang, J., Obersorster, G. and Biswas, P. (2009). "Characterization of Size, Surface Change, and Agglomeration State of Nanoparticle Dispersions for Toxicological Studies". *J Nanopart Res*, vol 11(1), pp 77-89
- Kannan, N. and Subbalaxmi, S. (2011). "Biogenesis of Nanoparticles – A Current Perspective". *Rev. Adv. Mater. Sci*, vol 27, pp 99-114
- Kaur, H., Kaur, S and Singh M. (2013). "Biosynthesis of Silver Nanoparticles by Natural Precursor from Clove and Their Antimicrobial Activity". *Biologia*, vol 68(6), pp 1048-1053
- Kim, K.J., Sung, W.S., Suh, B.K., Moon, S.K., Choi, J.S., Kim, J.G. and Lee, D.G. (2009). "Antifungal Activity and Mode of Action of Silver Nano-Particles on *Candida albicans*". *Biometals*, vol 22, pp 235-242
- Mondal, S., Mirdha, B.R. and Mahapatra, S.C. (2009). "The Science behind Sacredness of Tulsi (*Ocimum sanctum* Linn.)". *Indian J Physiol Pharmacol*, vol 53, pp 291-306
- Mukherjee, P., Ahmad, A., Mandal, D., Senapati, S., Sainkar, R.S., Khan, I.M., Parishcha, R., Ajaykumar, V.P., Alam, M., Kumar, R. and Sastry, M. (2001). "Fungus-Mediated Synthesis of Silver Nanoparticles and Their Immobilization in the Mycelia Matrix". *Nano Lett*, vol 1, pp 515-519
- Narasimha, G., Praveen, B., Mallikarjuna, K. and Raju, B.D.P. (2011). "Mushrooms (*Agaricus bisporus*) Mediated Biosynthesis of Silver Nanoparticles, Characterisation and Their Antimicrobial Activity". *Int. J. Nano Dimension*, vol 2, pp 29-36
- Pal, S., Tak, Y.K. and Song J.M. (2007). "Does The Antimicrobial Activity of Silver Nanoparticles Depend On The Shape of The Nanoparticle? A Study of the Gram-Negative Bacterium *Escherichia coli*". *Appl Environ Microbiol*, vol 73(6), pp 1712-1720

- Raseetha, V.S., Cheng, S.F. and Chuah, C.H. (2009). "Comparative Study of Volatile Compounds from Genus *Ocimum*". *Am J Appl Sci*, vol 6, pp 523-528
- Shahverdi A.R., Shakibaie, M. and Nazari, P. (2011). "Basic and Practical Procedures for Microbial Synthesis of Nanoparticles". *Metal Nanoparticles in Microbiology*, vol 1, pp 177-195
- Sharma, V.K., Yngard, R.A. and Lin, Y. (2009). "Silver Nanoparticles: Green Synthesis and Their Antimicrobial Activities". *Adv. Colloid Interface Sci*, vol 145, pp 83-96
- Sondi, I. and Salopek-Sondi, I. (2004). "Silver Nanoparticles as Antimicrobial Agent: A Case Study on *E. coli* as a Model for Gram Negative Bacteria". *J. Colloid Interface Sci*, vol 275, pp 177-182
- Sun, R.W., Chen, R., Chung, N.P., Ho, C.M., Lin, C.L. and Che, C.M. (2005). "Silver Nanoparticles Fabricated in Hepes Buffer Exhibit Cytoprotective Activities Toward HIV-1 Infected Cells". *Chem. Commun*, vol 40, pp 5059-5061
- Sun, S., Murray, C., Weller, D., Folks, L. and Moser A. (2000). "Monodisperse FePt Nanoparticles and Ferromagnetic FePt Nanocrystal Superlattices". *Nano Science*, vol 287(5460), pp 1989-1992